Slope Stability Engineering, Yagi, Yamagami & Jiang © 1999 Balkema, Rotterdam, ISBN 90 5809 079 5

Stability evaluation of sliding failure along thin mudstone deposit due to excavation

Y. Nakamura – *AICO Company Limited, Japan*
J. Kojima – *Tokai Technology Center, Japan*
S. Hanagata – *Wakachiku Construction Company Limited, Japan*
K. Narita & Y. Ohne – *Department of Civil Engineering, Aichi Institute of Technology, Toyota, Japan*

ABSTRACT: This paper concerns the mechanism of sliding failure along a thin layer of mudstone deposit due to excavation. Some laboratory tests were carried out on both undisturbed and reconstituted samples of the mudstone material to know its shear strength characteristics, especially on the relation among strength values of the peak, residual and normally consolidated states. Stability evaluation was then conducted by use of FEM and a conventional limit equilibrium approach in order to discuss accuracy and reliability of the estimated behavior of the clay slope as compared to that observed in the field during excavation.

1 INTRODUCTION

A large scale sliding failure happened to occur in a project of land improvement due to excavation. A thin layer of mudstone deposit of 5 to 10cm thick lies beneath deposits of clay and gravel mixture of about 10m thick, and a big slide took place through this thin mudstone layer immediately after excavation of talus and clay deposit, accompanying large horizontal and vertical deformation of the order of 50cm to 150cm. Field investigation and survey conducted after failure revealed that the mudstone deposit lies with a very low angle to the horizon and is considered to have some latent sliding planes which had been a cause of instability of the existing clay slope before excavation.

This paper concerns the mechanism of sliding failure along a thin layer of mudstone deposit due to excavation. Some laboratory tests were carried out on both undisturbed and reconstituted samples of the mudstone material to know its shear strength characteristics, especially on the relationship among strength values of the peak, residual and normally consolidated states. Material tests were also conducted on the clay deposit in order to estimate stress-strain behavior of slope during failure and lateral earth pressure acting in the field to promote sliding. Stability evaluation was then conducted by use of FEM and a simple conventional approach of limit equilibrium in order to discuss accuracy and reliability of the estimated behavior of the clay slope as compared to that observed in the field during excavation.

2 OUTLINE OF SLIDING FAILURE

The sliding failure now under consideration took place in a project of land improvement of about 32.5ha in area. The land has a topography of gentle slope hill formed near a river, of about 40m in height, as illustrated in a plan view in Figure 1 and in the cross-sectional view of A-A in Figure 2a). The profile of the hill is geologically composed of a Tertiary mudstone deposit of Neogene period as a bedrock, Tertiary deposits of porcelain clay and sand gravel overlying the bed, and a talus deposit of Quaternary on the hillside.

A big sliding failure of soil block of 150m wide, 120m long and 8 to 10m deep took place immediately after the excavation of a part of talus and porcelain clay deposit, along a thin flat layer of mudstone deposit inclined with a very low angle of 2 to 3 $^{\circ}$ to the horizontal. This mudstone deposit of 10 to 20cm thick lying beneath the porcelain clay differs a little from the bedrock deposit, containing some kind of carbide, and a thin layer of chocolate color alterated clay of 5 to 10cm thick is considered to be a potential slip surface in this sliding failure.

The sliding took place just after excavating the clay deposit in 5 to 7m, and a large deformation was observed, as indicated by displacement vectors of point survey in Figure 1, in the horizontal and vertical direction of the order of 50cm to 150cm in the duration of two months until a countermeasure construction is completed by replacing a part of soil near the toe of the slope with crashed stone, as shown in Figure 2c). The land slide is thus characterized by a very flat and straight slip of a soil block on along a polished latent sliding plane.

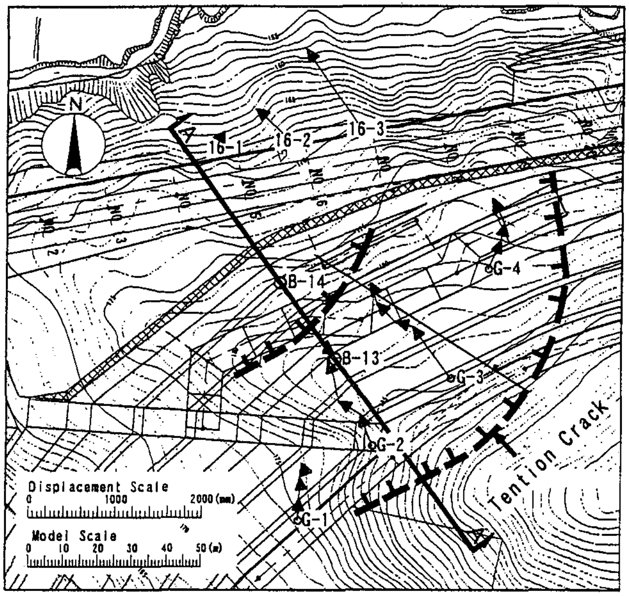

Figure 1. Plan view of sliding failure

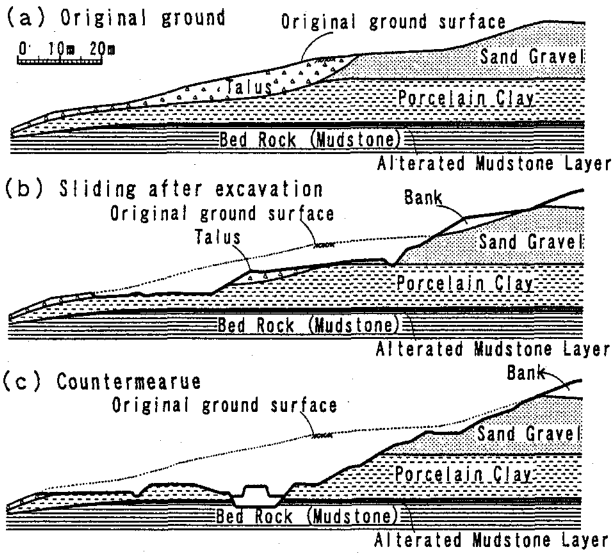

Figure 2. Cross sectional view along A-A

3 SHEAR STRENGTH CHARACTERISTICS OF ALTERATED MUDSTONE DEPOSIT

Laboratory shear strength tests were carried out on both the undisturbed and reconstituted samples of the alterated mudstone deposit to know its peak and the ultimate residual strength values. Some physical properties of the mudstone material are summarized in Table 1.

Table 1. Physical properties of mudstone

Density of solid particle:	2.71g/cm^3
Natural water content:	52.8%
Content of Sand:	4.2%
Silt:	30.6%
Clay:	65.2%
Liquid limit:	116.3%
Plastic limit:	31.1%
Plastic index:	85.2

3.1 *Repeated loading direct shear test*

In order to investigate the relationship between the peak and residual strength of the material, direct shear test was conducted on undisturbed samples by applying shear force repeatedly from one side to the other several times until the ultimate state of shear failure is reached. The test was done under CD condition: The sample was first submerged in a week to be saturated state and consolidated in 24 hours under a constant vertical pressure, and then loaded repeatedly up to ± 6mm in horizontal direction under a drained condition at the rate of 0.01mm/min..

Figure 3 shows an example of shear stress and deformation relation curve in a repeated loading under a vertical pressure of σ_v=200kPa. It is seen that shear stress gradually decreases nearly at a constant rate and tends to converge to a certain ultimate state as the repeated loading proceeds. The relation curves of shear stress and deformation are again plotted in Figure 4 by taking as usual the total absolute shear deformation on the abscissa. Point of interests noticed in this figure is the fact that the shear deformation until the peak strength is reached is significantly smaller as compared to that after peak to the ultimate state.

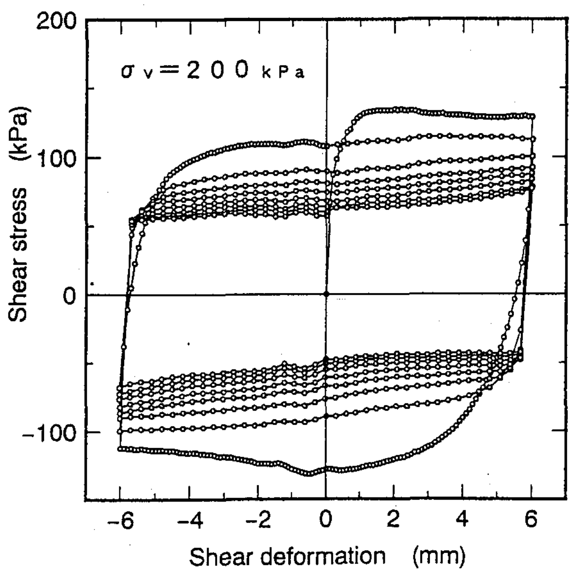

Figure 3. Stress-deformation in repeated loading

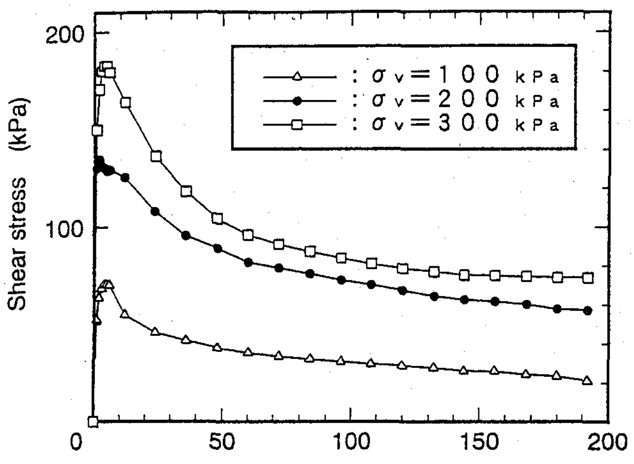

Figure 4. Shear stress vs. total deformation

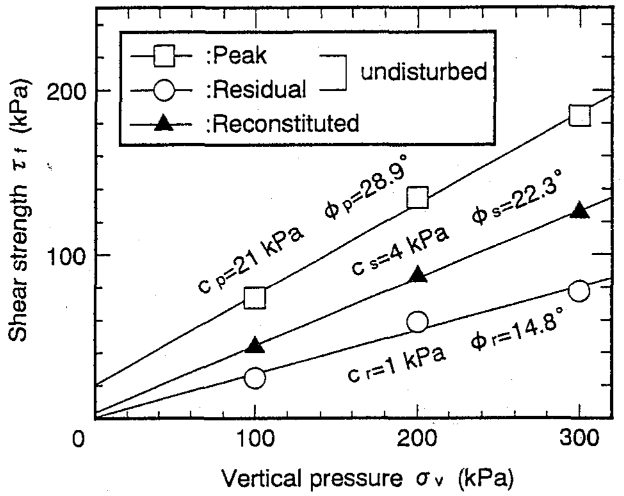

Figure 5. Comparison of failure lines

Failure lines are drawn for the peak and the residual strength in Figure 5, where the latter is defined here by the shear stress at deformation of 200mm. It should be noted that the undisturbed samples have a certain small amount of cohesion component in the peak strength, which is supposed to be constituted with its stress history in the field, but it disappears by a large shear deformation in the residual state.

3.2 *Direct shear test on reconstituted samples*

Direct shear strength tests were also carried out on the reconstituted slurry samples of the mudstone to compare the strength value obtained above with that at completely softened state. The slurry sample of under 0.42mm was consolidated in a week with its self weight and cut out and set in the shear box for a CD test under a specified vertical pressure. Shear stress and deformation curves obtained in the test are hyperbola in shape as usually observed in a normally consolidated clay and the maximum shear stress at a large deformation was defined here as the completely softened strength. Failure line thus determined for the reconstituted sample is drawn in Figure 5, indicating very small cohesion intercept, similarly as normally consolidated clay, and rather large angle of friction as compared to the residual strength of the undisturbed samples.

4 FEM ANALYSIS

In order to discuss stress and deformation behavior and safety against sliding along the thin mudstone deposit, a FEM elastic analysis of excavation is conducted on the cross section presented in Figure 2a), which was obtained through site investigation after failure. The solution of a simple self weight analysis for the model with the original ground surface before excavation is superposed with that by an inverse load due to excavation. Deformation parameters used in the analysis, some of them were determined from the results of triaxial tests, are taken to be 5MPa for the thin mudstone layer and 10 ~ 25MPa for overlain clay and gravel mixture.

Figure 6 shows distributions of the local factor of safety (F_s) obtained at elements along the surface of the thin mudstone layer for the original configuration before excavation. The factor F_s is defined here as a ratio of the radius of the stress circle at failure to that at the present state and was evaluated for three different cases of strength values (c, ϕ) presented in Figure 5; i.e., ① Peak and ② Residual strength of the undisturbed sample, and ③ NC (normally consolidated) strength of the reconstituted sample, respectively. Also shown in Figure 7 is distributions of F_s calculated for the configuration after excavation and filling of banks on the gravel layer. Distributions of the maximum shear stresses τ_{max} acting along the thin mudstone layer before and after excavation are also plotted in Figure 8, together with the change in stress circles before and after excavation at two representative elements of No.10 and No.20 below the toe of the first and the second step of the excavated slope, respectively.

Discussions associated with these figures are summarized in the following.

1) Distributions of F_s before excavation in Figure 6 are rather flat in shape for every case of (c, ϕ) under consideration. This suggests equal potential of sliding along the base, though the lowest value of F_s appears near the toe of the original slope in the case of residual strength.

2) Distributions of F_s after excavation in Figure 7

demonstrate locations of higher potential of sliding near the toe of the first and second step of the excavated slope. The value of F_S becomes below unity in the case of residual strength along two sections (1) and (2) near the above toes, where tension cracks were observed in the time sequence as the 1st(1) and the 2nd(2) slide in the field.

3) Distributions of τ_{max} in Figure 8, together with the change in stress states at No.10 and No.20 elements before and after excavation, suggest the occurrence of different patterns of failure along the

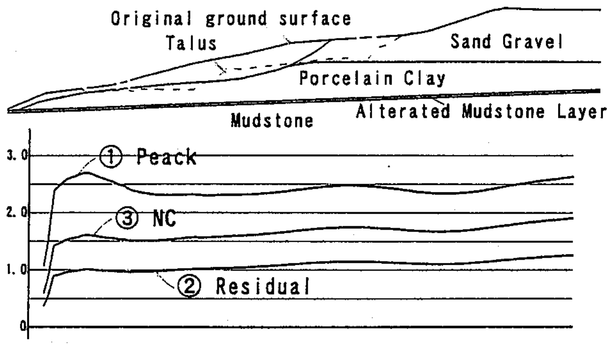

Figure 6. Distribution of F_S before excavation

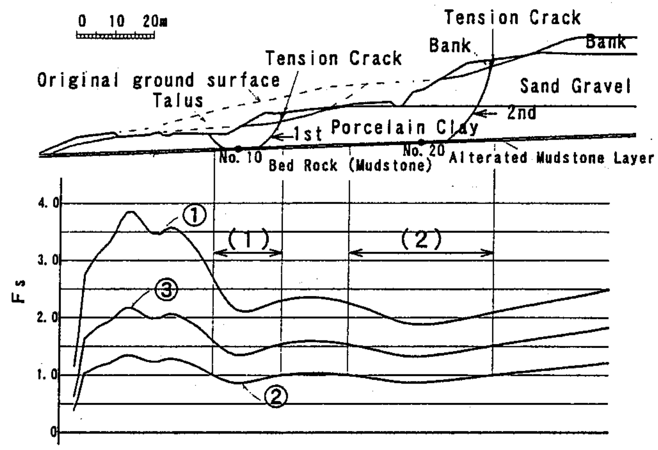

Figure 7. Distribution of F_S after excavation

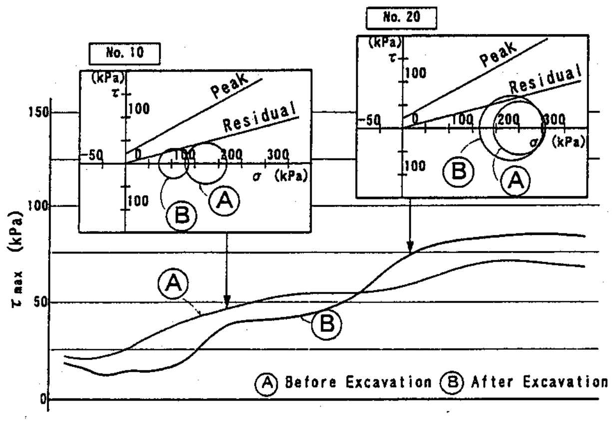

Figure 8. Stress change before and after excavation

slip plane: i.e., failure at No.10 element is largely dependent on the loss of confining pressure, not at least on the increase in shear stresses, and that at No.20 is mainly caused by an increase in shear stress accompanied by a significant unbalance of overburden weight due to excavation and filling.

4) Stability analysis was conducted by use of a limit equilibrium method for two composite sliding planes, which start in circles from the points where tension cracks were detected, running along straight surface of the mudstone layer, and passing through in circles again near No.10 element, as illustrated in Figure 7. The values of safety factor for the 1st small and the 2nd large sliding planes obtained in three cases of (c, ϕ) are listed in Table 2. Very low safety in the 1st slide, irrespective of strength values, suggests higher potential of a local sliding failure and is considered to be a threshold of the overall big failure due to excavation.

Table 2. Safety factor based on limit equilibrium

	① Peak	② Residual	③ NC
1st	1.13	0.35	0.61
2nd	2.03	0.75	1.23

Although much more discussion is still required on the mechanism of progressive nature of sliding failure, for instance presented by Bjerrum 1967 and Burland et al. 1977, some useful suggestions were supplied in this paper on the stability evaluation of sliding along a thin weak mudstone deposit.

5 CONCLUSIONS

FEM analysis can be a practically useful tool for evaluating stability of sliding failure along a thin mudstone deposit due to excavation, together with the residual strength obtained in the repeated loading direct shear test. Distributions of local factor of safety roughly indicate the position of higher potential of sliding and stress circles at elements along the failure plane suggest different patterns of failure, which are supposed reasonable to interpret sliding failure observed in the field.

REFERENCES

Bjerrum,L. 1967. Progressive failure in slopes of over-consolidated plastic clay and clay shales, *Proc ASCE, 93-SM5*: 3-49.

Burland,J.B. et al. 1977. A study of ground movement and progressive failure caused by a deep excavation in Oxford Clay, *Geotechnique, 27-4*: 557-591.